International Journal of Advanced Science and Technology
Vol. 29, No. 11s, (2020), pp. 1427-1430

Influence of implantation ions on the electronic structure of GaP(111) surface

Donaev S.B., Umirzakov B.E., Abduvayitov A.A.
Tashkent State Technical University named after Islam Karimov.
100095, str.2 University, Tashkent

Abstract

In this article, the relationship between the band gap E_g and the sizes of nanocrystalline phases is studied. It has been established that in the case of surface sizes of phases d *less than 35–40 nm (thickness 3.5–4 nm), quantum-size effects disappear in the Ga0.6Al0.4P nanocrystalline phases. The band gap of the $Ga_{0.6}Al_{0.4}P$ nanocrystalline phases, depending on their size, increases from 2.4 eV (at* d = *30-35 nm) to 3.1 eV (at* d = *10-12 nm).*
Keywords: *surface, single crystal, ion implantation, nanocrystalline phase, band gap, quantum-size effect.*

1. Introduction

Binary semiconductors A3B5 and multicomponent heterostructures based on them are widely used in the creation of various devices of opto-, micro- and nanoelectronics. In particular, multilayer structures with GaP, GaInP, AlGaInP layers are used and have prospects for the manufacture of laser diodes, solar cells, photoelectric and optoelectronic devices. Of particular interest is the preparation of ternary solid solutions of the $Ga_{1-x}AlxAs$, $Ga_xIn_{1-x}P$ type with an adjustable band gap. Therefore, to date, the composition, structure, electronic and optical properties of multicomponent and multilayer heterostructures based on A^3B^5 semiconductors have been well studied. [1-9]. Molecular beam and solid phase epitaxy methods are widely used to obtain such structures. Our studies conducted in recent years [10–13] showed that the low-energy ion implantation method is an effective means of creating nanoscale phases and layers on the surface and in the surface region of materials of various nature.

This work is devoted to the preparation of three-component nanophases and $Ga_{1-x}Al_xP$ nanofilms on the GaP surface by ion implantation and to the study of their composition, electronic and crystalline structure.

2. Experimental technique

Single crystal GaP (111) samples were chosen as objects of study. Before ion implantation, GaP (111) was degassed under ultrahigh vacuum ($P = 10^{-7}$ Pa) at T = 900 K for ~4 hours. The studies were carried out using the following methods: Auger electron spectroscopy (AES), spectroscopy of characteristic electron energy loss (SChEEL), ultraviolet photoelectron spectroscopy (UVES) and the removal of the energy and angular dependences of the secondary electron emission coefficients. To determine the depth distribution profile of atoms, a layer-by-layer Auger analysis was performed by sputtering the sample surface with 3 keV Ar^+ ions at an incidence angle of ~80-85° relative to the normal, the etching rate was трав (5 ± 1) Å/min. Ultraviolet photoelectron spectra were recorded at photon energies hν ≈ 10.8 eV. The photon source was a standard gas discharge hydrogen lamp.

3. Experiment Results

We previously found [14] that when GaP is bombarded with Al^+ ions with E_0 = 1 keV at a high dose ($D = 10^{17}$ cm^{-2}), Al atoms uniformly penetrate into the GaP surface region. In this case, the irradiated GaP layers are strongly disordered and the surface Al concentration is ~30-35 at.%. Table 1 shows the thickness of the GaAlP layer obtained by implantation of Al ions in GaP(111) with different energies at a dose of $D = D_{sat.}$ combined with annealing, as well as their band gap E_g and lattice constant a.

TABLE 1

E_0, keV	D, cm^{-2}	Composition	h, Å	E_g, eV	a, Å
0.5	$6 \cdot 10^{16}$	$Ga_{0.6}Al_{0.4}P$	20-25	2.34	5.45
1	10^{17}	$Ga_{0.6}Al_{0.4}P$	30-35	2.34	5.45
3	$2 \cdot 10^{17}$	$Ga_{0.6}Al_{0.4}P$	45-50	2.34	5.45
5	$2 \cdot 10^{17}$	$Ga_{0.7}Al_{0.3}P$	60-65	2.3	5.43

It is seen that with increasing E_0, the thickness of the three-component film increases. Up to E_0 = 3 keV, a single-crystal film is formed with an approximate composition of $Ga_{0.6}Al_{0.4}P$, and at E_0 = 5 keV, $Ga_{0.7}Al_{0.3}P$.

Figure 1 shows the spectra of the characteristic energy loss of electrons GaP(111) and GaP with a $Ga_{0.6}Al_{0.4}P$ surface film. It can be seen that the shape and intensity of the peaks of the surface and bulk plasmons of the studied samples are significantly different from each other, and their energy positions are not significantly different. This is probably due to the fact that when the gallium is partially replaced by aluminum, the number of valence electrons does not change much.

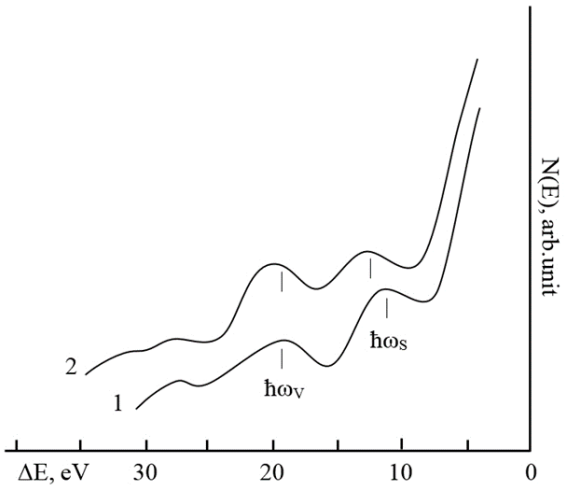

FIGURE: 1. Spectra of the characteristic energy loss of electrons for 1 - GaP(111); 2 - GaP(111) with a $Ga_{0.6}Al_{0.4}P$ film.

Figure 2 shows the angular dependence of inelastically reflected electrons η for pure GaP and GaP with a $Ga_{0.6}Al_{0.4}P$ film measured at Ep = 2000 eV.

It can be seen that the η(φ) curves of these samples are nonmonotonic and the position of the main peaks practically coincides with each other, i.e. it can be assumed that GaP and GaAlP have the same crystal structure with close lattice parameters. Studies using the RHEED method showed that the $Ga_{0.6}Al_{0.4}P$ film crystallizes into a cubic lattice with a lattice constant a = 5.45 Å.

Note that, at D $<10^{14}$ cm^{-2}, the $Ga_{0.6}Al_{0.4}P$ nanocrystalline phases were not clearly distinguished, and at D $\geq 10^{16}$ cm^{-2}, the boundaries of individual phases overlapped and a continuous film was formed.

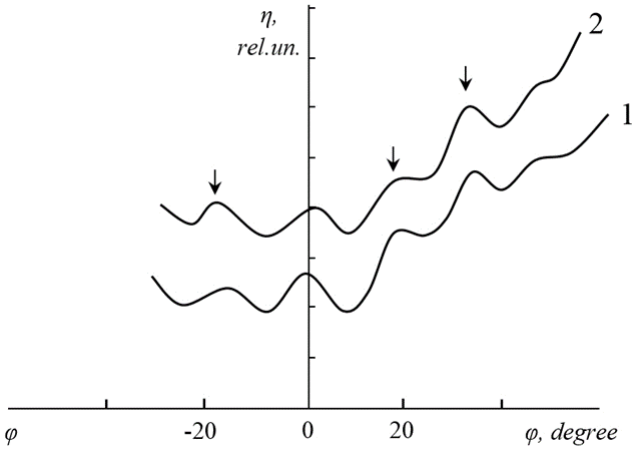

FIGURE: 2. Dependence of η on the angle of incidence φ of the primary electron beam for: 1 - GaP(111) single crystal, 2 - GaP(111) with a $Ga_{0.6}Al_{0.4}P$ film 35–40 Å thick

4. Conclusion

Thus, implantation of Al^+ ions with E_0 = 1 keV in GaP in combination with annealing yielded nanocrystalline phases (in the range $D = 5 \cdot 10^{14} - 8 \cdot 10^{15}$ cm^{-2}) and nanofilms (at $D = 4 \cdot 10^{16}$ cm^{-2}) $Ga_{0.6}Al_{0.4}P$ with a thickness h = 35–40 Å. It was shown that these phases and films crystallize into a cubic lattice and the lattice parameters approximately coincide with the GaP lattice parameters (a = 5.45 Å). The band gap of the $Ga_{0.6}Al_{0.4}P$ nanocrystalline phases, depending on their size, increases from 2.4 eV (at d = 30-35 nm) to 3.1 eV (at d = 10-12 nm).

References

[1]. T.N. Zavaritskaya, A.V. Kvit, N.N. Mel'nik and V.A. Karavanskii. The structure of porous gallium phosphide // Semiconductors, 1998, volume 32, pp.213–217. doi.org/10.1134/1.1187548

[2]. V.F. Agekyan, V.I. Ivanov-Omskii, V.N. Knyazevskii, V.Yu. Rud and Yu.V. Rud. Optoelectronic phenomena in GaAs and GaP layers prepared by nitrogen treatment // Semiconductors, 1998, volume 32, pp**.** 1075–1076. doi.org/10.1134/1.1187570

[3]. P.V. Seredin, E.P. Domashevskaya, I.N. Arsentyev, D.A. Vinokurov, A.L. Stankevich and T. Prutskij Superstructured ordering in $Al_xGa_{1-x}As$ and $Ga_xIn_{1-x}P$ alloys // Semiconductors, 2013, volume 47, pp. 1–6. https://doi.org/10.1134/S106378261301020X

[4]. Su-Huai Wei, A. Zunger. Optical properties of zinc-blende semiconductor alloys: Effects of epitaxial strain and atomic ordering // Phys.Rev. B, 1994, 49, 14337 doi.org/10.1103/PhysRevB.49.14337.

[5]. O.I. Ryumantsev, P.N. Brunkov, E.V. Pirogov and A.Yu. Egorov. Study of defects in heterostructures with GaPAsN and GaPN quantum wells in the GaP matrix // Semiconductors, 2010, volume 44, pp. 893-897. doi.org/10.1134/S1063782610070110

[6]. P.R.C. Kent and A. Zunger. Theory of electronic structure evolution in GaAsN and GaPN alloys // Phys.Rev. B, 2001, 64, 115208. doi.org/10.1103/PhysRevB.64.115208

[7]. M.A. Putyato, N.A. Valisheva, M.O. Petrushkov, V.V. Preobrazhenskii, I.B. Chistokhin and others. A Lightweight Flexible Solar Cell Based on a Heteroepitaxial InGaP/GaAs Structure // Technical Physics, 2019, volume 64, pp. 1010–1016(2019), doi.org/10.1134/S106378421907020X

[8]. M.A. Green, K. Emery, Ya. Hishikaw, W. Warta, E.D. Dunlop, D.H. Levi and A.W.Y. Ho-Baillie // Prog. Photovolt.: Res. Appl., 2016, Vol.25.N 1.P.3-13. DOI: 10.1002/pip.2855

[9]. A.F. Dyadenchuk and V.V. Kidalov. The use of porous A3B5 compounds for supercapacitor plates // Journal of Nano- and Electronic Physics, 2015, Volume 7, No. 1, 01021 (4cc) (in Russian).
[10]. B.E.Umirzakov, T.S.Pugacheva, A.T.Tashatov, D.A.Tashmukhamedova. Electronic structure and optical properties of CaF_2 films under low energy Ba^+ ion-implantation combined with annealing // Nuclear Instruments and Methods in Physics Research. Section B, Beam Interactions with Materials and Atoms; Journal Volume: 166-167, 2000; Journal Issue: 1-4, https://doi.org/10.1016/S0168-583X(99)01151-9 .
[11]. Z.A.Isakhanov, Z.E.Mukhtarov, B.E.Umirzakov, M.K.Ruzibaeva. Optimum ion implantation and annealing conditions for stimulating secondary negative ion emission // Technical Physics V.56, 546 (2011), doi.org/10.1134/S1063784211040177.
[12]. S.B.Donaev, F.Djurabekova, D.A.Tashmukhamedova, B.E.Umirzakov. Formation of nanodimensional structures on surfaces of GaAs and Si by means of ion implantation. Physica status solidi (c)12 (1-2), 89-93, doi.org/10.1002/pssc.201400156.
[13]. Kh.Kh.Boltaev, D.A.Tashmukhamedova, B.E.Umirzakov. Structure and electronic properties of nanoscale phases and nanofilms of metal silicides produced by ion implantation in combination with annealing // Journal of Surface Investigation. X-ray, Synchrotron and Neutron Techniques vol.8, pp.326–331(2014), doi.org/10.1134/S1027451014010108.
[14]. S.B. Donaev, B.E. Umirzakov. The effect of implantation of Al^+ ions on the composition, electronic and crystalline structure of the GaP (111) surface // Physics and Technology of Semiconductors, 2020, Issue 8, pp. 716-719. DOI: 10.21883/FTP.2020.08.49655.9399 (in Russian).